A&A 528, A121 (2011)
DOI: 10.1051/0004-6361/201015932

Astronomy & Astrophysics

Atmospheric parameters of red giants in the *Kepler* field⋆,⋆⋆

H. Bruntt[1], S. Frandsen[1], and A. O. Thygesen[1,2]

[1] Department of Physics and Astronomy, Aarhus University, 8000 Aarhus C, Denmark
e-mail: srf@phys.au.dk
[2] Nordic Optical Telescope, Apartado 474, 38700 Santa Cruz de La Palma, Santa Cruz de Tenerife, Spain

Received 14 October 2010 / Accepted 29 November 2010

ABSTRACT

Context. Accurate fundamental parameters of stars are mandatory for the asteroseismic investigation of the *Kepler* mission to succeed.
Aims. We determine the atmospheric parameters for a sample of six well-studied bright K giants to confirm that our method produces reliable results. We then apply the same method to 14 K giants that are targets of the *Kepler* mission.
Methods. We used high-resolution, high signal-to-noise ratio spectra acquired using the FIES spectrograph on the Nordic Optical Telescope. We applied the iterative spectral synthesis method VWA to derive the fundamental parameters from carefully selected high-quality iron lines and pressure-sensitive Calcium lines.
Results. We find good agreement with parameters from the literature for the six bright giants. We compared the spectroscopic values with parameters based on photometric indices in the Kepler Input Catalogue (KIC). We identify serious problems with the KIC values for [Fe/H] and find a large RMS scatter of 0.5 dex. The $\log g$ values in KIC agree reasonably well with the spectroscopic values displaying a scatter of 0.25 dex after excluding two low-metallicity giants. The $T_{\rm eff}$ values from VWA and KIC agree well with a scatter of about 85 K. We also find good agreement with $\log g$ and $T_{\rm eff}$ derived from asteroseismic analyses for seven *Kepler* giant targets.
Conclusions. We determine accurate fundamental parameters of 14 giants using spectroscopic data. The large discrepancies between photometric and spectroscopic values of [Fe/H] emphasize the need for further detailed spectroscopic follow-up of the *Kepler* targets. This will be mandatory to be able to produce reliable constraints for detailed asteroseismic analyses and interpretation of possible exo-planet candidates found around giant stars.

Key words. asteroseismology – stars: abundances – stars: fundamental parameters – stars: Population II

1. Introduction

During 2009, the space missions CoRoT and *Kepler* generated a high level of activity in the groups specialized in the asteroseismic analysis of photometric time series of stars. In both cases, the very long, continuous observing and the very low noise of the data acquired has opened up a completely new world of possibilities for the asteroseismic investigation of stellar interiors.

In particular, the seismic investigation of K giants has taken a huge leap forward. The results from a time series analysis of 150 days of measurements obtained by the CoRoT space telescope increased the number of known pulsating giants from a handful to nearly 800 (De Ridder et al. 2009). The *Kepler* mission will be observing the flux continuously of thousands of stars for at least 3 years and has increased both the number, the range in luminosity, and the length of the time series relative to data acquired by CoRoT. The high-precision light curves from *Kepler* constitute important data for detailed asteroseismic investigations of red giants because of the long temporal coverage and low noise levels of the observations. This has extended the range of giants with detected oscillations to lower luminosities (Bedding et al. 2010; Stello et al. 2010; Mosser et al. 2010).

Before we can hope to make a successful analysis of individual red giant stars observed by *Kepler*, we need however to measure accurate atmospheric parameters as discussed by Brown et al. (1994), Creevey et al. (2007), and Creevey (2009).

We have started the observations of about 100 *Kepler* red giant stars with the FIbre-fed Echelle Spectrograph (FIES) at the Nordic Optical Telescope (NOT). From the spectral analysis, we can determine accurate atmospheric parameters, which are essential for constraining the stellar models when comparing asteroseismic observations and theory. We concentrate in particular on old, metal poor stars, which are important for the understanding of the early history of the Galaxy. With our sample we will be able to present important insights into the observed variation in the pulsational behaviour with metallicity.

At present, only photometric determinations of metallicity are available, which are based on the Kepler Input Catalogue (Latham et al. 2005). The KIC is a photometric catalogue with estimated parameters of all stars down to $V \simeq 18$ in the *Kepler* field of view. The values of [Fe/H] have been shown to be inaccurate (Molenda-Żakowicz et al. 2010a,b), and we confirm this finding here.

2. Target selection

We selected a sample of stars with a range of luminosities and metallicities, according to the KIC. Our target stars are in quite

⋆ Based on observations made with the Nordic Optical Telescope, operated on the island of La Palma jointly by Denmark, Finland, Iceland, Norway, and Sweden, in the Spanish Observatorio del Roque de los Muchachos of the Instituto de Astrofisica de Canarias.

⋆⋆ Reduced spectra are only available in electronic form at the CDS via anonymous ftp to cdsarc.u-strasbg.fr (130.79.128.5) or via
http://cdsarc.u-strasbg.fr/viz-bin/qcat?J/A+A/528/A121

advanced stages of evolution and the effects of the assumed physics in the theoretical models are pronounced. The lifetimes of the modes are long enough to permit asteroseismic extraction of information from individual modes. The amplitudes of the modes and the large and small frequency separations for stars on the giant branch have already been measured (Bedding et al. 2010). However, more sophisticated diagnostics will become available when the duration of the time series is extended.

In the solar-metallicity open cluster M 67 (Stello et al. 2007), oscillations have been shown to be present in a few cases, while no evidence of oscillations have been seen in the metal-poor globular cluster M4 (Frandsen et al. 2007). It is indeed possible that low metallicity may lead to smaller pulsation amplitudes (Stello & Gilliland 2009). To verify this hypothesis and explore the metal dependency of the oscillations, we chose a set of targets with a wide spread in metallicity. The metal poor stars are at the same time among the oldest stars in the Galaxy. The determination of accurate ages from the asteroseismic analysis is therefore of special interest. The KIC contains a small number of possibly metal-poor K giants, but as mentioned the metallicity from the catalogue is very uncertain.

To verify that our adopted technique is valid, we analysed six bright K giant targets. They were selected from the work of Smith & Ruck (2000) and from the PASTEL catalogue (Soubiran et al. 2010) with the criterion that they have accurate values and represent a relatively wide range of atmospheric parameters.

3. The observations

We used spectra from a small pilot program carried out with the FIES spectrograph at the NOT in 2008, followed by a larger project in 2009, where five nights were allocated. Unfortunately, the number of spectra obtained in 2009 was small because of bad weather. In 2010, we have been much more successful (7 nights allocated), and the data for 50 giant stars are now being processed.

The spectrograph was used in the high resolution mode (R = 65 000) and ThAr calibration spectra were acquired both before and after each target exposure. The exposure-meter[1] was used to get similar signal-to-noise ratios (S/N) for all spectra in the range at 80−100. Exposure times varied from a few minutes for the brighter giants to one hour for fainter targets divided into two half-hour exposures to reduce problems with cosmic rays.

The extraction was done with the software package FIEStool[2] using the calibration frames recorded every night as is the standard procedure at the NOT.

4. Spectroscopic determination of atmospheric parameters

The high-resolution spectra obtained were used to determine the $T_{\rm eff}$, microturbulent velocity ($\xi_{\rm t}$), $\log g$, $v \sin i$, and metallicity of the selected sample of giants. For the analysis, we used iron lines in the wavelength range from 4500 Å to 7000 Å, avoiding the regions affected by telluric lines. The number of lines used depended on the S/N of the individual spectra and the degree of blending between neighboring lines. As far as possible, non-blended lines were preferred, resulting in rather few lines (≈40) for some of the targets in the sample.

[1] See http://www.not.iac.es/instruments/fies/

[2] See http://www.not.iac.es/instruments/fies/fiestool/FIEStool.html

4.1. Atmospheric parameters from Fe I/Fe II-abundances

We used the VWA software (Bruntt et al. 2004, 2008, 2010a,b) to determine the fundamental parameters of the targets. The software is a semi-automatic package in which a careful continuum normalization is done by manually selecting continuum points in the stellar spectrum by comparing it to a synthetic spectrum with similar fundamental parameters (Bruntt et al. 2010b). This was followed by a careful selection of the least blended lines, each of which were iteratively fitted with a synthetic spectrum, including the contribution from weakly blending lines. This is important for the rich giant spectra, especially in the blue wavelength range. We adopted MARCS model atmospheres (Gustafsson et al. 2008) and atomic line data from the Vienna Atomic Line Database (Kupka et al. 1999). Each line fit was inspected in great detail and poor fits discarded, resulting in between 40−120 Fe I and 3−11 Fe II lines being used in the determination of the fundamental parameters. As initial guesses of the parameters of the model atmosphere, the values in the KIC were used. The $\xi_{\rm t}$ and $T_{\rm eff}$ parameters were then refined through several iterations to remove correlations between the abundances of Fe I and respectively, equivalent width (EW) and excitation potential (EP). We also insisted on agreement between the Fe I and Fe II abundances during the model fitting by adjusting $T_{\rm eff}$ and $\log g$. An example of the Fe I abundances versus EW and EP is shown in Fig. 1 for a giant with high, solar, and low metallicity. We note that abundances are measured relative to the same lines in the solar spectrum, as described by Bruntt et al. (2010b).

The results for the 14 giants are presented in Table 1. All abundances are measured relative to the Sun, with the errors being represented by the RMS scatter in the abundances of each line included in the fit. The uncertainties in $T_{\rm eff}$, $\log g$, and $\xi_{\rm t}$ were calculated by changing one model parameter at a time, until at least a 3-σ difference was produced in the Fe I/Fe II abundances or in the slope of the abundances versus either EP or EW. From these, a 1-σ error was calculated, giving the internal precision of the parameters calculated in VWA. To this, we quadratically added a systematic error that we evaluate in Sect. 4.4, using the results for the six bright giants.

4.2. Log g from pressure sensitive lines

It is possible, especially for cool stars, to determine $\log g$ from a selection of strong, pressure-sensitive lines, thus placing additional constraints on the surface gravity. Commonly used lines are the Mg Ib, Na I D, and the Ca I lines at 6122 Å and 6162 Å. Determination of $\log g$ for giants from the Mg Ib and Na I D lines was problematic since the degree of line blending or the S/N in these areas did not enable us to make a trustworthy continuum determination. In addition, the Mg Ib lines are so wide and lie so close that there is no continuum present between them, making the normalization even more difficult. Furthermore, we found that these lines are quite insensitive to changes in the surface gravity. We therefore only used the Ca lines for the $\log g$ determination. In some cases, the degree of line blending around one of the Ca lines was so severe that a reliable fit could not be made, thus only one Ca line was used to estimate the $\log g$ value. For a single target (KIC 4157282), this was the case for both Ca lines, so only the matching Fe I/Fe II abundances could be used.

An example of fitting the Ca 6162 line is shown in Fig. 2. The observed spectrum around the Ca lines was compared with three synthetic spectra, each with a different value of $\log g$. The χ^2 value was then calculated for each fit to determine the best value for $\log g$. The method is described in greater detail by

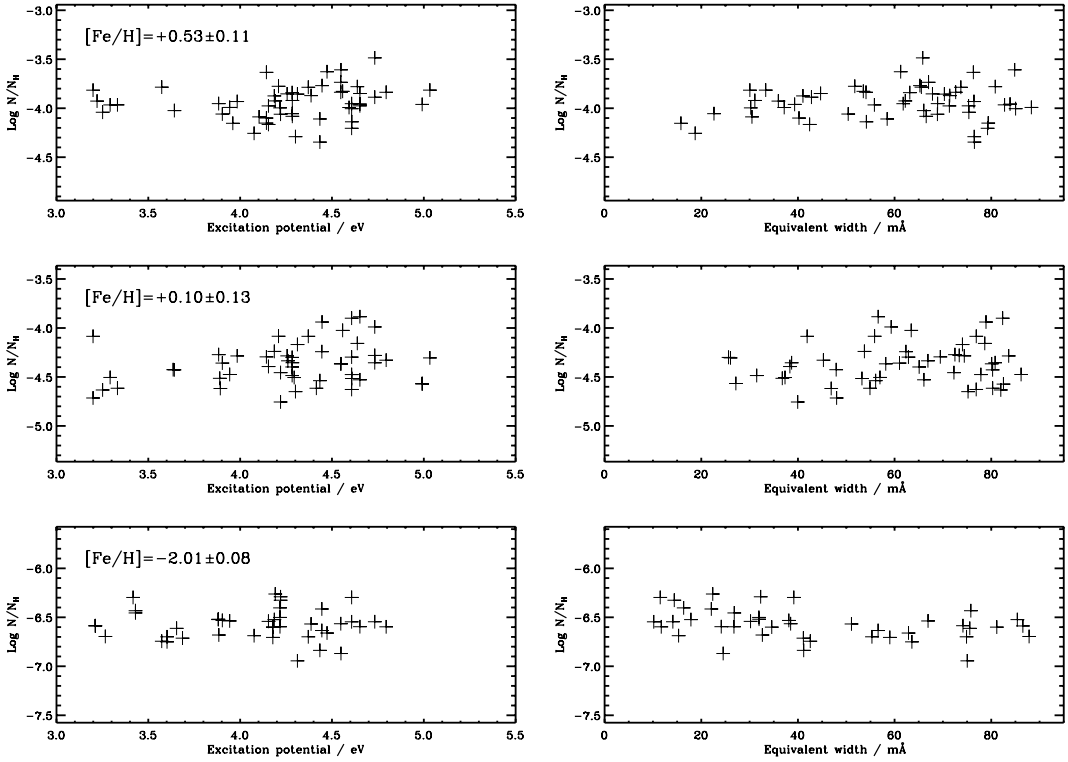

Fig. 1. Examples of diagnostic plots of Fe I abundance versus excitation potential and equivalent width for three different giants with KIC-IDs 11342694, 4157282, and 8017159 (*top to bottom*).

Table 1. Atmospheric parameters of the 14 *Kepler* K giant targets as determined from VWA.

KIC-ID	$T_{\rm eff}$	$\log g$ (Fe I/Fe II)	$\log g$ (Ca λ6122)	$\log g$ (Ca λ6162)	$\langle \log g \rangle$
1726211	4950 ± 70	2.29 ± 0.10	–	2.80 ± 0.26	2.36 ± 0.26
2714397	5000 ± 70	2.68 ± 0.08	2.23 ± 0.44	2.48 ± 0.31	2.65 ± 0.25
3744043	5020 ± 70	3.06 ± 0.07	3.16 ± 0.18	3.10 ± 0.15	3.08 ± 0.25
3860139	4550 ± 90	2.61 ± 0.20	1.98 ± 0.20	2.20 ± 0.09	2.23 ± 0.25
3936921	4580 ± 90	2.11 ± 0.17	–	2.27 ± 0.17	2.19 ± 0.27
4157282	4450 ± 90	1.88 ± 0.26	–	–	1.88 ± 0.35
4177025	4390 ± 90	1.93 ± 0.22	–	1.74 ± 0.25	1.85 ± 0.29
5709564	4775 ± 70	2.48 ± 0.09	2.15 ± 0.34	2.47 ± 0.11	2.46 ± 0.25
7006979	4770 ± 70	2.22 ± 0.06	–	2.52 ± 0.31	2.23 ± 0.25
8017159	4625 ± 70	1.11 ± 0.08	2.21 ± 0.28	–	1.19 ± 0.25
8476245	4865 ± 70	1.86 ± 0.09	2.24 ± 0.21	–	1.92 ± 0.25
10403036	4485 ± 70	1.90 ± 0.18	–	2.02 ± 0.09	2.00 ± 0.25
10426854	4955 ± 80	2.38 ± 0.15	2.46 ± 0.47	2.73 ± 0.22	2.49 ± 0.27
11342694	4695 ± 100	3.10 ± 0.18	2.52 ± 0.19	2.46 ± 0.26	2.75 ± 0.27

KIC-ID	[Fe/H]	$\xi_{\rm t}$ [km s^{-1}]	$v_{\rm macro}$ [km s^{-1}]	$v \sin i$ [km s^{-1}]	$v_{\rm rad}$ [km s^{-1}]
1726211	−0.66 ± 0.08	1.36 ± 0.40	4.0 ± 1.0	0.5 ± 1.0	−145.1 ± 0.5
2714397	−0.40 ± 0.08	1.40 ± 0.25	3.5 ± 1.0	1.5 ± 1.0	−191.6 ± 0.5
3744043	−0.25 ± 0.08	1.10 ± 0.14	1.5 ± 1.0	3.0 ± 1.0	−55.3 ± 0.5
3860139	+0.25 ± 0.13	1.35 ± 0.50	4.0 ± 1.0	2.5 ± 1.0	−25.2 ± 0.5
3936921	+0.29 ± 0.10	1.15 ± 0.56	5.0 ± 1.0	2.0 ± 1.0	−48.6 ± 0.5
4157282	+0.10 ± 0.13	0.97 ± 0.21	3.0 ± 1.0	2.5 ± 1.0	−36.7 ± 0.5
4177025	−0.25 ± 0.11	1.40 ± 0.40	2.0 ± 1.0	2.0 ± 1.0	−123.5 ± 0.5
5709564	−0.22 ± 0.08	1.50 ± 0.08	4.3 ± 1.0	1.0 ± 1.0	−105.9 ± 0.5
7006979	−0.36 ± 0.08	1.50 ± 0.16	4.0 ± 1.0	1.2 ± 1.0	−57.4 ± 0.5
8017159	−2.01 ± 0.08	1.70 ± 0.30	3.0 ± 1.0	3.0 ± 1.0	−376.0 ± 0.5
8476245	−1.33 ± 0.09	1.85 ± 0.28	3.0 ± 1.0	3.0 ± 1.0	−130.4 ± 0.5
10403036	−0.58 ± 0.09	1.35 ± 0.09	2.0 ± 1.0	4.5 ± 1.0	−125.7 ± 0.5
10426854	−0.31 ± 0.10	1.45 ± 0.23	2.0 ± 1.0	3.3 ± 1.0	−45.7 ± 0.5
11342694	+0.53 ± 0.11	0.93 ± 0.26	2.0 ± 1.0	3.7 ± 1.0	−20.0 ± 0.5

Notes. The $\log g$ value is determined from the Fe I/Fe II ionization balance and the wide Ca lines at λ6122 and λ6162 Å. These measurements are combined and the weighted mean is given as $\langle \log g \rangle$.

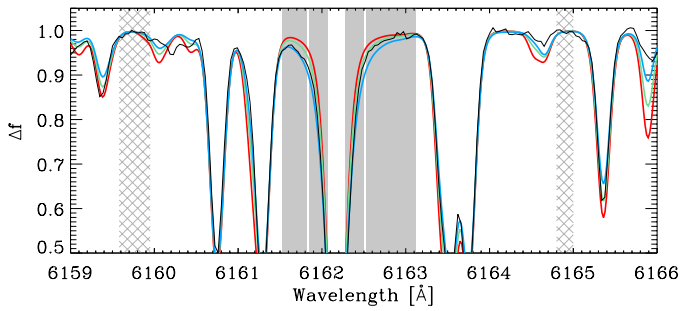

Fig. 2. Example of fitting the pressure-sensitive Ca line at 6162 Å in Arcturus (α Boo). Hatched regions are used to normalise the spectrum and χ^2 is calculated in the four shaded regions. The best fit is the green line; the red/blue line has $\log g$ lower/higher by 0.6 dex.

Bruntt et al. (2010b). The best-fit values for $\log g$ are quoted in Table 1, where the weighted mean of the determination from the Fe I/Fe II abundances and the Ca lines is taken as the final result, and given in the last column.

4.3. Determination of $v \sin i$ and macroturbulence

To estimate the values of $v \sin i$ and macroturbulence, we evaluated by visual inspection the fits of synthetic line profiles to dozens of isolated lines throughout the spectrum. The results quoted in Table 1 were taken as the average of the values found from the individual fits. It is seen that both the macroturbulence and $v \sin i$ for the giants is more or less the same and the surface rotation is very slow as expected for giant stars. The uncertainty in the parameters was estimated by changing the parameters until a significant deviation from the observed profile was seen in the fit. The deviation was found by visual inspection of the fitted line profiles and is thus only a rough estimate of the uncertainty.

4.4. Discussion

To validate our method, we obtained FIES spectra of six bright giants, chosen from the works of Soubiran et al. (2010) and Smith & Ruck (2000). Soubiran et al. (2010) used the TGMET method for their analysis, where a large grid of spectra from the ELODIE spectrograph are assigned parameters from an extensive literature search. The parameters of each star are then found by locating the most closely matching spectrum in the library. We compare the results in Fig. 3 and Table 3. There are no significant offsets for $\log g$ or $T_{\rm eff}$ between the TGMET method and VWA, although our [Fe/H] values are slightly higher by about 0.1 dex. The RMS scatter of the differences is 60 K for $T_{\rm eff}$, 0.24 dex for $\log g$, and 0.07 dex for [Fe/H]. We adopt these as the "systematic errors" caused by the differences in the adopted method, grid of model atmospheres, spectrum normalization etc. We are aware that a rigorous treatment of each of these effects would require a much larger sample of stars, and is beyond the scope of this work.

An analysis of the *Kepler* light curves has already been carried out for seven of the targets in our sample (Kallinger et al. 2010). This analysis gives values of $T_{\rm eff}$ and $\log g$ and relies on the comparison of the asteroseismic data with an evolutionary model grid. As seen in Fig. 4, there is good agreement between the $\log g$ values found using VWA and the values from the asteroseismic analysis. However, the comparison of $T_{\rm eff}$ in the lower panel shows a correlation with $T_{\rm eff}$, which may indicate a systematic problem in the approach of Kallinger et al. (2010) for the hottest giants. The mean offsets and RMS values

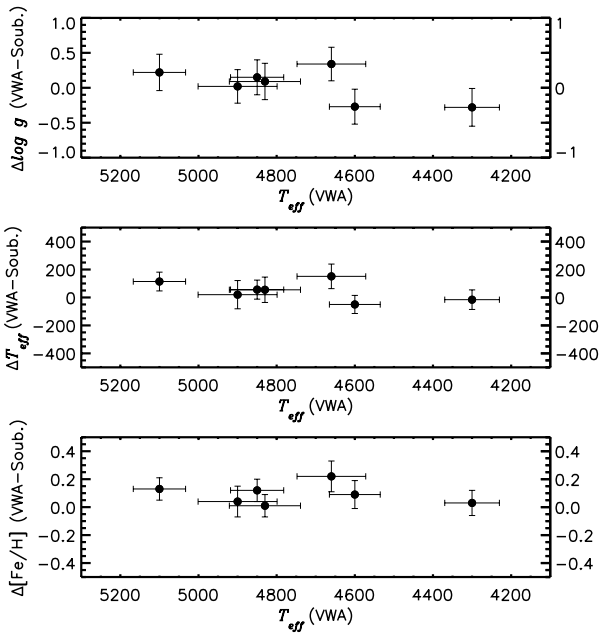

Fig. 3. Comparison of parameters determined from VWA and the PASTEL catalogue (Soubiran et al. 2010) for six bright giants.

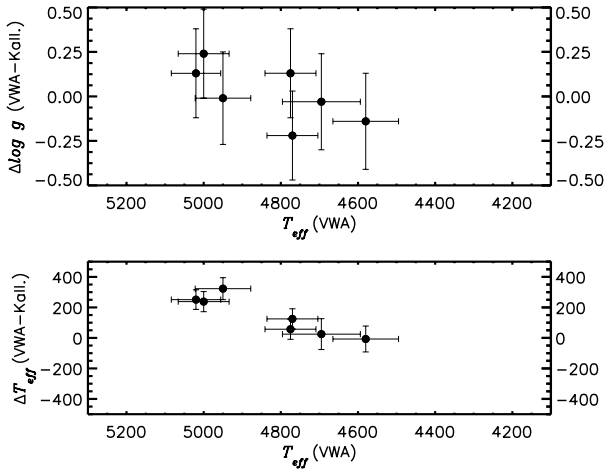

Fig. 4. Comparison of $\log g$ and $T_{\rm eff}$ determined from VWA and the asteroseismic method of Kallinger et al. (2010).

are $\Delta \log g = 0.01 \pm 0.27$ dex and $\Delta T_{\rm eff} = 145 \pm 127$ K, respectively. The asteroseismic values are tabulated in Table 2 along with the parameters from the KIC.

In Fig. 5 and Table 2, we compare the atmospheric parameters from KIC with the VWA analysis (left panels) and the spectroscopic study of Molenda-Żakowicz et al. (2010b) (right panels). The two studies show the same overall picture, but our sample includes significantly more of the evolved stars with $T_{\rm eff} < 4800$ K. We now discuss the comparison of VWA and the KIC values. A large scatter is clearly evident when comparing [Fe/H] from VWA and KIC: the range is from −1 to +1 dex with the average difference and RMS scatter being Δ[Fe/H] = +0.10 ± 0.50. For $\log g$, we note that the two stars with the largest discrepancy also have the lowest metallicity (KIC-IDs 8017159 and 8476245), which may represent a problem in KIC for the low-metallicity stars. If we consider only the remaining one dozen stars, we obtain $\Delta \log g = -0.05 \pm 0.25$,

Table 2. Comparison of the spectroscopic parameters from VWA with photometric values from KIC and from the asteroseismic analysis of 14 *Kepler* giants.

	VWA			KIC			Asteroseis.	
KIC-ID	$T_{\rm eff}$	$\log g$	[Fe/H]	$T_{\rm eff}$	$\log g$	[Fe/H]	$T_{\rm eff}$	$\log g$
1726211	4950±70	2.36 ± 0.26	−0.66 ± 0.08	4837 ± 200	2.68 ± 0.50	−0.96 ± 0.50	4627±103	2.37 ± 0.04
2714397	5000±70	2.65 ± 0.25	−0.40 ± 0.08	4881 ± 200	2.52 ± 0.50	−0.53 ± 0.50	4762±99	2.41 ± 0.01
3744043	5020±70	3.08 ± 0.25	−0.25 ± 0.08	4994 ± 200	2.50 ± 0.50	−0.09 ± 0.50	4769±115	2.95 ± 0.02
3860139	4550±90	2.23 ± 0.25	+0.25 ± 0.13	4589 ± 200	2.22 ± 0.50	+0.60 ± 0.50		
3936921	4580±90	2.19 ± 0.27	+0.29 ± 0.10	4436 ± 200	2.38 ± 0.50	−0.06 ± 0.50	4587±54	2.33 ± 0.04
4157282	4450±90	1.88 ± 0.35	+0.10 ± 0.13	4344 ± 200	2.13 ± 0.50	−0.78 ± 0.50		
4177025	4390±90	1.85 ± 0.29	−0.25 ± 0.11	4346 ± 200	2.14 ± 0.50	−0.49 ± 0.50		
5709564	4775±70	2.46 ± 0.25	−0.22 ± 0.08	4752 ± 200	2.52 ± 0.50	−0.06 ± 0.50	4718±118	2.33 ± 0.04
7006979	4770±70	2.23 ± 0.25	−0.36 ± 0.08	4891 ± 200	2.21 ± 0.50	−0.01 ± 0.50	4645±103	2.45 ± 0.05
8017159	4625±70	1.19 ± 0.25	−2.01 ± 0.08	4634 ± 200	2.45 ± 0.50	−1.07 ± 0.50		
8476245	4865±70	1.92 ± 0.25	−1.33 ± 0.09	4817 ± 200	2.76 ± 0.50	−1.20 ± 0.50		
10403036	4485±70	2.00 ± 0.25	−0.58 ± 0.09	4388 ± 200	2.21 ± 0.50	−1.39 ± 0.50		
10426854	4955±80	2.49 ± 0.27	−0.31 ± 0.10	4731 ± 200	2.57 ± 0.50	−1.03 ± 0.50		
11342694	4695±100	2.75 ± 0.27	+0.53 ± 0.11	4603 ± 200	2.65 ± 0.50	+0.50 ± 0.50	4670±90	2.78 ± 0.02

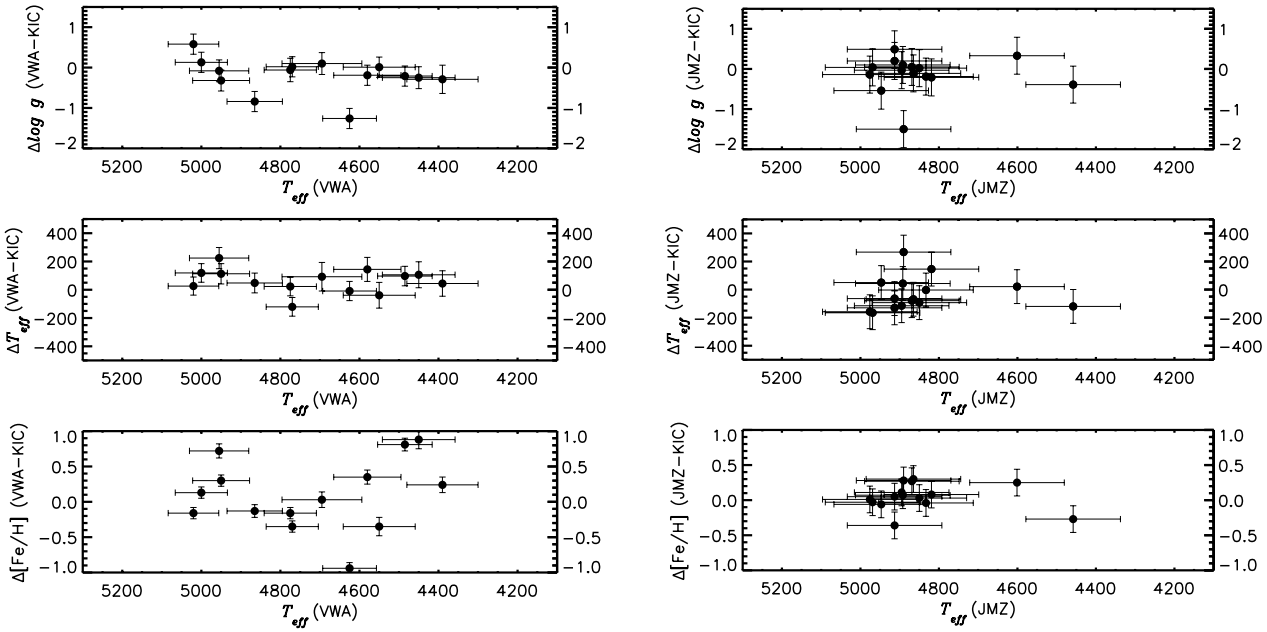

Fig. 5. *Left panels*: comparison of atmospheric parameters determined with VWA and from KIC. *Right panels*: comparison of atmospheric parameters determined with ROTFIT (Molenda-Żakowicz et al. 2010b) and KIC.

Table 3. Comparison of parameters from VWA and the PASTEL catalogue (Soubiran et al. 2010) for six bright giants.

	VWA			Pastel		
ID	$T_{\rm eff}$	$\log g$	[Fe/H]	$T_{\rm eff}$	$\log g$	[Fe/H]
α Mon	4850 ± 70	2.77 ± 0.25	+0.08 ± 0.08	4794	2.62	−0.04
μ Leo	4660 ± 90	2.63 ± 0.24	+0.53 ± 0.11	4509	2.29	+0.31
α Boo	4300 ± 70	1.43 ± 0.27	−0.52 ± 0.09	4316	1.71	−0.55
λ Peg	4830 ± 90	2.56 ± 0.26	−0.08 ± 0.08	4775	2.47	−0.09
μ Peg	5100 ± 70	2.96 ± 0.26	+0.05 ± 0.08	4986	2.74	−0.08
ψ UMa	4600 ± 70	2.11 ± 0.25	−0.04 ± 0.10	4605	2.38	−0.13

Notes. Uncertainties on $T_{\rm eff}$, $\log g$, and [Fe/H] for PASTEL are 80 K, 0.1 dex and 0.1 dex, respectively.

which indicates that the KIC values are fairly robust. Finally, the spectroscopic effective temperatures are in fairly good agreement with the KIC values, $\Delta T_{\rm eff} = +62 \pm 85$ K.

From our sample of 14 Kepler giants, we conclude that the KIC values for $T_{\rm eff}$ and $\log g$ are trustworthy for target selection and statistical studies of their asteroseismic properties, but only for [Fe/H] > -0.5 dex. It is clear that for detailed asteroseismic analyses we need homogeneously determined spectroscopic parameters.

5. Conclusion

We have determined accurate atmospheric parameters for a sample of 14 K-giant targets that are being observed with the NASA *Kepler* satellite. These parameters are mandatory to place constraints on asteroseismic models when comparing observations

and theory. We have confirmed the results of Molenda-Żakowicz et al. (2010a,b) that there are serious discrepancies for [Fe/H] when comparing with the photometric KIC catalogue (RMS scatter in [Fe/H] of 0.5 dex), while $T_{\rm eff}$ and $\log g$ values are in reasonable agreement. However, for $\log g$ we find discrepancies of about 1 dex for two stars with [Fe/H] < -1.0, indicating that there may be a problem in the KIC catalogue at low metallicities.

We have validated our method and evaluated the systematic errors by analysing the spectra of six bright giants with well-known parameters and compared our results with the literature, confirming that our analysis is reliable. We have also found good agreement between our parameters and the ones found from asteroseismology.

The uncertainties in $\log g$ and [Fe/H] in KIC are too large to match the quality of the data produced by *Kepler*, emphasizing the importance and need for further, detailed spectroscopic studies of the *Kepler* giant targets. This paper will be followed by a second paper presenting the results for an additional 50 K giants.

We have verified that one of the *Kepler* giants is a population II star (KIC 8017159), and we expect to find several more in our larger sample of stars. Until now, only one nearby population II star, ν Ind, has been studied using asteroseismic techniques (Bedding et al. 2006).

Acknowledgements. We are grateful for the many useful comments from Dennis Stello and to Thomas Kallinger for sharing results from his asteroseismic analyses. This research took advantage of the SIMBAD and VIZIER databases at the CDS, Strasbourg (France), and NASA's Astrophysics Data System Bibliographic Services.

References

Bedding, T. R., Butler, R. P., Carrier, F., et al. 2006, ApJ, 647, 558
Bedding, T. R., Huber, D., Stello, D., et al. 2010, ApJ, 713, L176
Brown, T. M., Christensen-Dalsgaard, J., Weibel-Mihalas, B., & Gilliland, R. L. 1994, ApJ, 427, 1013
Bruntt, H., Bikmaev, I. F., Catala, C., et al. 2004, A&A, 425, 683
Bruntt, H., De Cat, P., & Aerts, C. 2008, A&A, 478, 487
Bruntt, H., Bedding, T. R., Quirion, P., et al. 2010a, MNRAS, 405, 1907
Bruntt, H., Deleuil, M., Fridlund, M., et al. 2010b, A&A, 519, A51
Creevey, O. L. 2009, in ASP Conf. Ser. 416, ed. M. Dikpati, T. Arentoft, I. González Hernández, C. Lindsey, & F. Hill, 363
Creevey, O. L., Monteiro, M. J. P. F. G., Metcalfe, T. S., et al. 2007, ApJ, 659, 616
De Ridder, J., Barban, C., Baudin, F., et al. 2009, Nature, 459, 398
Frandsen, S., Bruntt, H., Grundahl, F., et al. 2007, A&A, 475, 991
Gustafsson, B., Edvardsson, B., Eriksson, K., et al. 2008, A&A, 486, 951
Kallinger, T., Mosser, B., Hekker, S., et al. 2010, A&A, 522, A1
Kupka, F., Piskunov, N., Ryabchikova, T. A., Stempels, H. C., & Weiss, W. W. 1999, A&AS, 138, 119
Latham, D. W., Brown, T. M., Monet, D. G., et al. 2005, in BAAS, 37, 1340
Molenda-Żakowicz, J., Bruntt, H., Sousa, S., et al. 2010a, Astron. Nachr., 331, 981
Molenda-Żakowicz, J., Jerzykiewicz, M., Frasca, A., et al. 2010b [arXiv:1005.0985]
Mosser, B., Belkacem, K., Goupil, M., et al. 2010, A&A, 517, A22
Smith, G., & Ruck, M. J. 2000, A&A, 356, 570
Soubiran, C., Le Campion, J., Cayrel de Strobel, G., & Caillo, A. 2010, A&A, 515, A111
Stello, D., & Gilliland, R. L. 2009, ApJ, 700, 949
Stello, D., Bruntt, H., Kjeldsen, H., et al. 2007, MNRAS, 377, 584
Stello, D., Basu, S., Bruntt, H., et al. 2010, ApJ, 713, L182